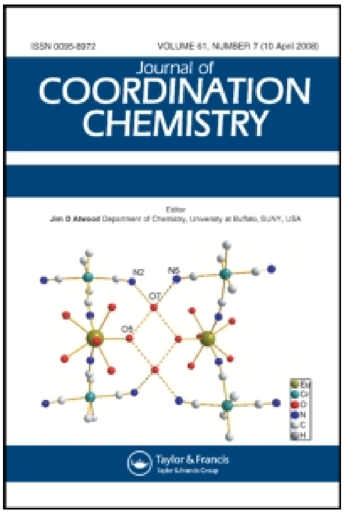

Journal of Coordination Chemistry
Publication details, including instructions for authors and subscription information:
http://www.informaworld.com/smpp/title~content=t713455674

Synthesis and pH-sensitive redox properties of 1,10-phenanthroline-5,6-dione complexes

Ying-Ying Kou[a]; Guang-Jun Xu[b]; Wen Gu[a]; Jin-Lei Tian[a]; Shi-Ping Yan[a]
[a] Department of Chemistry, Nankai University, Tianjin, P.R. China [b] Bethune Military Medical College, Forth Military Medical University, Shijiazhuang, P.R. China

To cite this Article Kou, Ying-Ying , Xu, Guang-Jun , Gu, Wen , Tian, Jin-Lei and Yan, Shi-Ping(2008) 'Synthesis and pH-sensitive redox properties of 1,10-phenanthroline-5,6-dione complexes', Journal of Coordination Chemistry, 61: 19, 3147 — 3157

To link to this Article: DOI: 10.1080/00958970802010575

URL: http://dx.doi.org/10.1080/00958970802010575

Journal of Coordination Chemistry
Vol. 61, No. 19, 10 October 2008, 3147–3157

Taylor & Francis
Taylor & Francis Group

Synthesis and pH-sensitive redox properties of 1,10-phenanthroline-5,6-dione complexes

YING-YING KOU†, GUANG-JUN XU‡, WEN GU†,
JIN-LEI TIAN† and SHI-PING YAN*†

†Department of Chemistry, Nankai University, Tianjin, P.R. China
‡Bethune Military Medical College, Forth Military Medical University,
Shijiazhuang, P.R. China

(*Received 5 October 2007; in final form 5 December 2007*)

Synthesis and pH-sensitive electrochemical properties of three complexes, $[Cu(PD)_3]\cdot(ClO_4)_2\cdot 2.25CH_3CN\cdot 6H_2O$ (**1**), $[Cu(PD)(DMSO)Cl_2]\cdot DMSO\cdot H_2O$ (**2**) and $[Co(PD)_3]\cdot(ClO_4)_2\cdot CH_3CN\cdot 2H_2O$ (**3**) (PD=1,10-phenanthroline-5,6-dione), are reported. Single-crystal X-ray diffraction of the complexes suggest that the structure of **1** is orthorhombic, **2** triclinic and **3** orthorhombic. The electrochemical properties of free PD and the three complexes in phosphate buffer solutions in a pH range between 2 and 9 have been investigated using cyclic voltammetry. The redox potentials of these compounds are strongly dependent on the proton concentration in the range $-0.3\,V \sim 0.4\,V$ *versus* SCE (saturated calomel reference electrode). The reduction behavior of PD can be described from quinone species to semiquinone anion then to the fully reduced dianion. At $pH < 4$, the reduction of PD proceeds via $2e^-/3H^+$ processes, while at $pH > 4$, the reduction of PD proceeds via $2e^-/2H^+$. For all complexes, the N–N chelate PD ligand is electrochemically active and underwent step reduction via $2e^-/2H^+$.

Keywords: 1,10-Phenanthroline-5,6-dione; Copper(II); Cobalt(II); Cyclic voltammetry

1. Introduction

The transition metal complexes containing redox active ligands display remarkable photochemical and electrophysical properties. Especially, complexes with dioxolene ligands have been intensively studied [1–3] because dioxolene takes three oxidation states: quinone, semiquinone and catecholate. Complexes containing semiquinone and catecholate have been shown to support intramolecular electron transfer [4–6] or between localized metal and quinone electronic levels within the semiquinone/catecholate complex molecule [7, 8]. Coordination of quinone ligands in monometallic systems would give additional electrochemical activity at potentials near the redox potentials of the metals [9]. We chose PD as ligand because it has interesting

---

*Corresponding author. Email: yansp@nankai.edu.cn

Journal of Coordination Chemistry
ISSN 0095-8972 print/ISSN 1029-0389 online © 2008 Taylor & Francis
DOI: 10.1080/00958970802010575

electrochemistry property [7] and it is a N–N chelate ligand containing an o-quinoid moiety, exhibiting pH-dependent responses. Owing to its redox activity, free PD and ruthenium, cobalt, iron, and nickel complexes show strong electrocatalytic activity for oxidation of NADH [10, 11]. We focused on the development of mononuclear transition metal complexes of 1,10-phenanthroline-5,6-dione: copper(II) and cobalt(II) complexes, such as $[Cu(PD)_3]\cdot(ClO_4)_2\cdot 2.25CH_3CN\cdot 6H_2O$ (**1**), $[Cu(PD)(DMSO)Cl_2]\cdot DMSO\cdot H_2O$ (**2**) and $[Co(PD)_3]\cdot(ClO_4)_2\cdot CH_3CN\cdot 2H_2O$ (**3**) and investigated their electrochemical properties and the influence of acidity.

2. Experimental

2.1. *Materials and measurements*

All reagents were obtained from Tianjin Guangfu Chemical Reagent Company and used without further purification. The reagents used were analytical reagent grade. Elemental analyses (C, H, N) were carried out on a Perkin-Elmer 240 analyzer.

2.2. *Electrochemistry*

Cyclic voltammetry measurements were performed on a BAS Epsilon Electrochemical Workstation. All samples were purged with argon prior to measurements. A standard three-electrode system consisting of a glassy carbon working electrode, a platinum-wire counter electrode and a saturated calomel reference electrode (SCE) was used. All potentials are referenced to the saturated calomel reference electrode without consideration of the liquid junction potential. The sweep rate during the CV measurements was $100\,mV\,S^{-1}$. Acidic solutions in a pH range between 2 and 4 were adjusted by mixing $0.1\,mol\,dm^{-3}$ $HClO_4$ and $0.1\,mol\,dm^{-3}$ NaH_2PO_4 solutions. The phosphate buffer solutions in a pH range between 4 and 9 were prepared using $0.1\,mol\,dm^{-3}$ NaH_2PO_4, $0.1\,mol\,dm^{-3}$ Na_2HPO_4 and $0.1\,mol\,dm^{-3}$ Na_3PO_4 solutions. The pH measurements were carried out using a WTW-315i pH meter (Wissenchaftlich-Technische Werkstätten Instruments Inc.).

2.3. *X-ray crystallography*

A green single crystal of $[Cu(PD)_3]\cdot(ClO_4)_2\cdot 2.25CH_3CN\cdot 6H_2O$ (**1**) with approximate dimensions of $0.04\times 0.02\times 0.02\,mm^3$, a grass green single crystal of $[Cu(PD)(DMSO)Cl_2]\cdot DMSO\cdot H_2O$ (**2**) with approximate dimensions of $0.22\times 0.18\times 0.16\,mm^3$ and a yellow single crystal of $[Co(PD)_3]\cdot(ClO_4)_2\cdot CH_3CN\cdot 2H_2O$ (**3**) with approximate dimensions of $0.26\times 0.19\times 0.08\,mm$ were mounted on glass fibers. Determination of the unit cells and data collection were performed using Mo-Kα radiation ($\lambda = 0.71073\,Å$) on a Bruker SMART 1000 diffractometer equipped with a CCD camera. The ω–φ scan technique was employed [12]. Crystal parameters and structure refinements for the complexes are summarized in table 1. Selected bond lengths and angles are listed in table 2. The structures were solved primarily by direct methods and secondly by Fourier difference techniques and refined using the

Table 1. Crystal data and structure refinement for **1**, **2** and **3**.

Complex	**1**	**2**	**3**
Empirical formula	$C_{40.50}H_{24.75}Cl_2N_{8.25}O_{14}$	$C_{16}H_{20}Cl_2CuN_2O_5S_2$	$C_{38}H_{25}Cl_2CoN_7O_{16}$
Formula weight	985.38	518.90	965.48
Temperature (K)	113(2)	294(2)	293(2)
Wavelength (Å)	0.71073	0.71073	0.71073
Crystal system	Orthorhombic,	Triclinic	Orthorhombic
Space group	*P*2(1)2(1)2(1)	$P\bar{1}$	*P*2(1)2(1)2(1)
Unit cell dimensions (Å, °)			
a	13.839(3)	7.1283(10)	13.876(2)
b	14.101(4)	13.1464(18)	14.238(2)
c	20.637(5)	13.1593(19)	20.763(3)
α	90.00	61.288(2)	90
β	90.00	76.072(2)	90
γ	90.00	86.593(2)	90
Volume (Å^3), *Z*	4027.1(17), 4	1074.5(3), 2	4101.9(11), 4
Calculated density (Mg m^{-3})	1.625	1.645	1.563
Absorption coefficient (mm^{-1})	0.758	1.527	0.631
F(000)	2002	530	1964
Crystal size (mm^3)	0.04 × 0.02 × 0.02	0.22 × 0.18 × 0.14	0.26 × 0.19 × 0.08
θ range for data collection (°)	1.75 to 25.00	1.77 to 25.02	1.73 to 25.03
Reflections collected/unique	7105/5692 [$R_{int} = 0.072$]	5470/3684 [$R_{int} = 0.0190$]	22426/7229 [$R_{int} = 0.0236$]
Completeness $\theta = 26.41$	99.9%	99.3%	99.9%
Goodness-of-fit on F^2	1.08	1.027	0.973
Final *R* indices [$I > 2\sigma(I)$]	$R_1 = 0.0667$, $wR_2 = 0.1327$	$R_1 = 0.0310$, $wR_2 = 0.0768$	$R_1 = 0.0502$, $wR_2 = 0.1084$
R indices (all data)	$R_1 = 0.0872$, $wR_2 = 0.1444$	$R_1 = 0.0406$, $wR_2 = 0.0825$	$R_1 = 0.1037$, $wR_2 = 0.1236$
Largest diff. peak and hole (e Å^{-3})	0.34 and −0.60	0.430 and −0.339	0.426 and 0.284

Table 2. Selected bond lengths (Å) and angles (°) for **1**, **2** and **3**.

Complex	Bond lengths (Å)		Bond angles (°)	
1	Cu1–N5	2.078 (6)	N5–Cu1–N1	174.4 (2)
	Cu1–N1	2.102 (6)	N5–Cu1–N3	95.1 (2)
	Cu1–N3	2.121 (6)	N1–Cu1–N3	88.87 (19)
	Cu1–N4	2.128 (4)	N5–Cu1–N4	90.01 (19)
	Cu1–N6	2.130 (6)	N1–Cu1–N4	94.6 (2)
2	Cu1–O3	1.9988 (19)	O3–Cu1–N2	88.04 (8)
	Cu1–N2	2.035 (2)	O3–Cu1–N1	164.81 (8)
	Cu1–N1	2.033 (2)	N2–Cu1–N1	80.36 (8)
	Cu1–Cl1	2.5080 (8)	O3–Cu1–Cl2	92.80 (6)
	Cu1–Cl2	2.2603 (8)	N1–Cu1–Cl2	93.94 (6)
3	Co1–N5	2.103 (4)	N5–Co1–N1	89.29 (16)
	Co1–N1	2.118 (4)	N5–Co1–N6	77.81 (18)
	Co1–N6	2.119 (5)	N1–Co1–N6	95.14 (16)
	Co1–N4	2.124 (5)	N5–Co1–N4	95.16 (17)
	Co1–N2	2.127 (5)	N1–Co1–N4	174.32 (18)

full-matrix least squares method. Computations were performed with the SHELXL-97 program [13, 14]. All non-hydrogen atoms were refined anisotropically. The hydrogen atoms were set in calculated positions and refined as riding atoms with a common fixed isotropic thermal parameter.

2.4. *General procedure for the synthesis of (1), (2) and (3)*

1,10-Phenanthroline-5,6-dione was prepared according to the literature method [15].

$[Cu(PD)_3]\cdot(ClO_4)_2\cdot2.25CH_3CN\cdot6H_2O$ (**1**) was prepared by mixing a CH_3CN (10 mL) solution of $Cu(ClO_4)_2\cdot6H_2O$ (186 mg, 0.5 mmol) with 1,10-phenanthroline-5,6-dione (105 mg, 0.5 mmol) in CH_3CN (5 mL) solution, the solution was refluxed for two hours, filtered and evaporated at room temperature. Green prism single crystals suitable for X-ray diffraction were obtained after one month. Yield: 45%. Calcd for $C_{40.50}H_{24.75}Cl_2CuN_{8.25}O_{14}$ (%): C, 49.13; H, 2.40; N, 11.61. Found (%): C, 49.32; H, 2.51; N, 11.72.

$[Cu(PD)(DMSO)Cl_2]\cdot DMSO\cdot H_2O$ (**2**) was prepared by mixing a water (5 mL) solution of $CuCl_2\cdot2H_2O$ (171 mg, 0.5 mmol) with 1,10-phenanthroline-5,6-dione (0.5 mmol) in DMSO (5 mL) solution, the solution was stirred overnight at room temperature, filtered and evaporated at room temperature. Grass green blocky single crystals suitable for X-ray diffraction were obtained on slow evaporation of a DMSO-H_2O solution of the complex after five months. Yield: 85%. Calcd for $C_{16}H_{20}Cl_2CuN_2O_5S_2$ (%): C, 37.35; H, 3.77; N, 5.51. Found (%): C, 37.03; H, 3.88; N, 5.40.

$[Co(PD)_3]\cdot(ClO_4)_2\cdot CH_3CN\cdot2H_2O$ (**3**) was synthesized by mixing a water (5 mL) solution of $Co(ClO_4)_2\cdot6H_2O$ (183 mg, 0.5 mmol) with 1,10-phenanthroline-5,6-dione (0.5 mmol) in methanol (5 mL), the solution stirred for 10 min at room temperature, the yellow precipitate filtered off and dissolved in CH_3CN. Yellow blocky single crystals suitable for X-ray diffraction were obtained on slow evaporation of a mixed solution of the complex after 10 days. Yield: 55%. Calcd for $C_{38}H_{25}Cl_2CoN_7O_{16}$ (%): C, 47.44; H, 2.50; N, 10.14. Found (%): C, 47.27; H, 2.61; N, 10.16.

Caution! Perchlorate salts of metal complexes containing organic ligands are potentially explosive. Only small quantity of material should be prepared and handled with suitable safety measures.

3. Results and discussion

The metal complexes were characterized by X-ray structural analyses. The electrochemical properties of free PD, **1**, **2** and **3** in aqueous solutions at various pH values were investigated.

3.1. *X-ray structural characterization*

The perspective view of $[Cu(PD)_3]\cdot(ClO_4)_2\cdot2.25CH_3CN\cdot6H_2O$ (**1**) is shown in figure 1; key bond lengths and angles are summarized in table 2. In the complex, copper(II) is coordinated by six nitrogen atoms to form a distorted octahedron. N1, N3, N5, N6 are nearly coplanar, while the axial coordination sites are occupied by N2 and N4. The copper is shifted by 0.0457 Å from the equatorial plane. The Cu–N distances are 2.102(6), 2.121(6), 2.078(6) and 2.130(6) Å in the equatorial plane, while 2.152(5) and 2.128(4) Å for the axial. The bond angle of N2–Cu1–N4 is 169.6(2)°.

The perspective view of $[Cu(PD)(DMSO)Cl_2]\cdot DMSO\cdot H_2O$ (**2**) is shown in figure 2. The key bond lengths and angles are summarized in table 2. In the complex, the

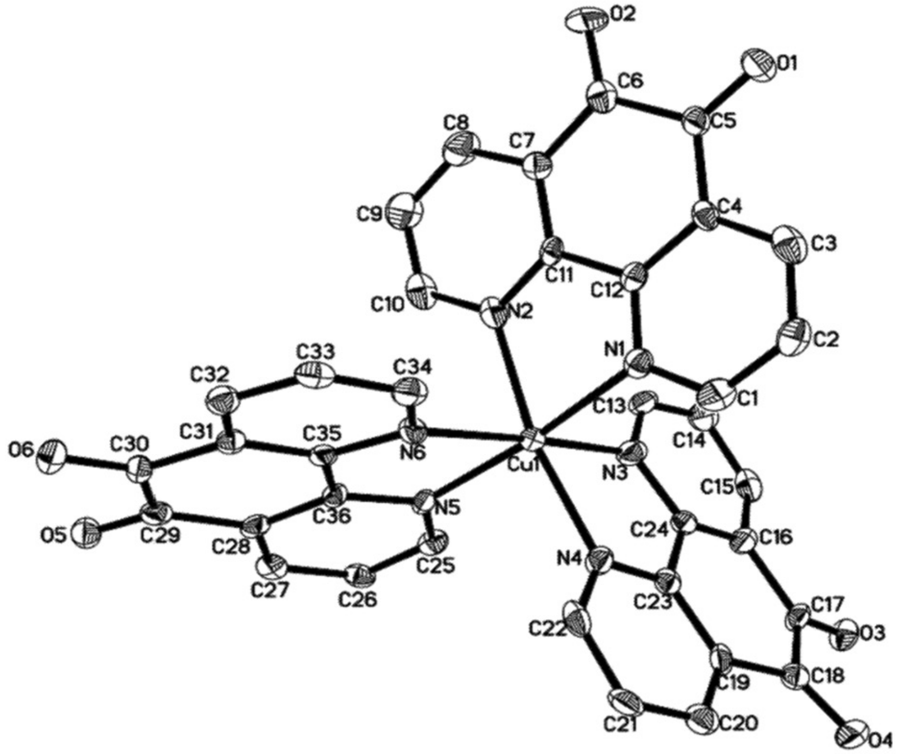

Figure 1. ORTEP diagram of **1**.

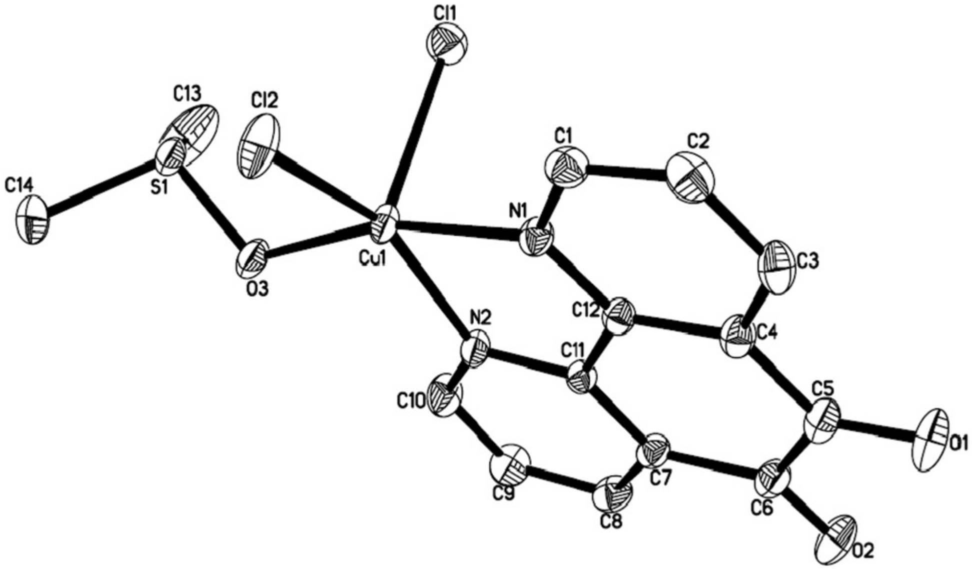

Figure 2. ORTEP diagram of **2**.

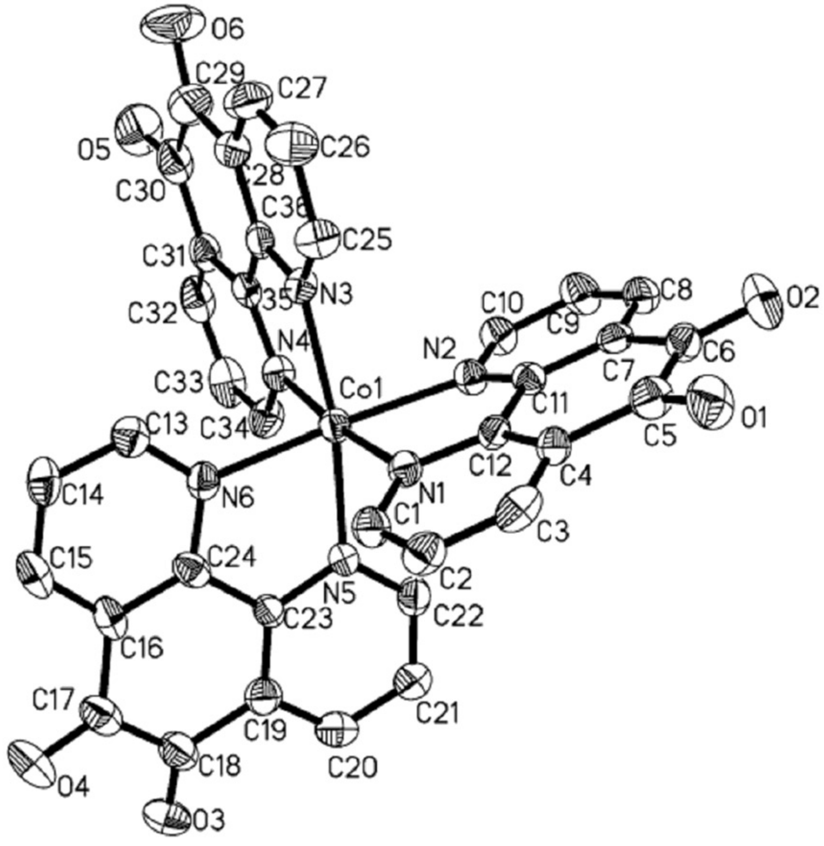

Figure 3. ORTEP diagram of **3**.

copper(II) is coordinated in a distorted square pyramidal geometry through the DMSO oxygen O3, two N atoms of PD and Cl2 in the basal plane and Cl1 in the apical position. The four equatorial donor atoms are nearly coplanar, while the copper atom is 0.3229 Å out of the plane. As is usual, the Cu1–Cl1 distance of 2.5080(8) Å is significantly longer than Cu1–Cl2 2.2603(8) Å.

The structure of $[Co(PD)_3] \cdot (ClO_4)_2 \cdot CH_3CN \cdot 2H_2O$ (**3**) is shown in figure 3. The key bond lengths and angles are summarized in table 2. In the complex, the cobalt(II) is coordinated by six nitrogen atoms to form a distorted octahedron. N1, N2, N4 and N6 are nearly coplanar, while the cobalt atom is 0.0380 Å out of the plane. The axial coordination sites are occupied by N3 and N5. The Co–N distances are 2.118(4), 2.124(5), 2.129(4) and 2.119(5) Å in the equatorial plane, while 2.127(5) and 2.103(4) Å in the axial. The N3–Co1–N5 bond angle is 169.44(16)°.

3.2. *Cyclic voltammetric studies*

In order to facilitate electrochemical assignments of the metal–PD complexes, the electrochemistry of free PD will be briefly discussed; the cyclic voltammogram

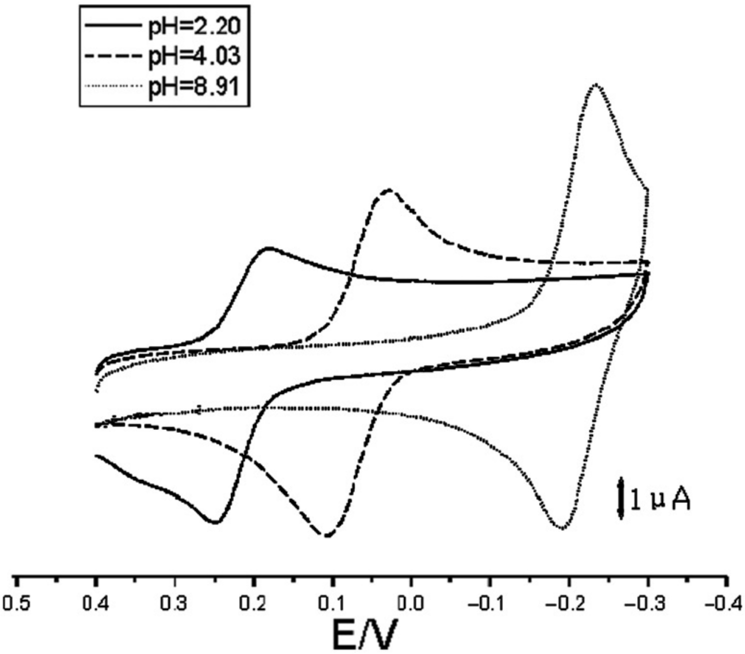

Figure 4. Cyclic voltammograms of PD in 0.1 mol L^{-1} phosphate buffer solutions at several pH values.

for the free ligand was obtained under the same conditions as those employed in study of its complexes. Figure 4 shows the cyclic voltammogram of PD in different pH phosphate buffer solutions. The voltammograms exhibit a couple of redox peaks with peak potential shifted to the more negative values as pH increases; studies at $pH > 9$ are made difficult by the base-catalyzed decomposition of PD, which produces 4,5-diazafluorenone. The broad anodic and cathodic waves at low pH are interpreted as overlap of two closely successive (quinone/semiquinone) and (semiquinone/catecholate) redox couples [Equations (1) and (2)] [16]. This assumption, supported by their peak potentials, was irrespective of the scan rates. The ΔE_p of ~42 mV was obtained at high pH, which is attributed to reduction of the quinone species to the semiquinone anion followed by reduction to the fully reduced dianion at the same potential [17].

Figure 5 shows the plot of E_c values of free PD against pH. There is a breakpoint at ca pH 4, and the slopes of the plot below pH 4 and above pH 4 were determined graphically as ca −83 and −54 mV/pH, respectively. The slopes in the plot indicate that the reduction of the PD occurs via $2e^-/3H^+$ and $2e^-/2H^+$ processes [17]. Thus, quinone molecules undergo two one-electron reductions in H_2O to give catecholate analogues and simultaneously combine one or two protons [Equations (1) and (2)].

In the range of pH 2–4, the pyridine nitrogen site of PD was protonated [Equation (3)] [18].

The electrochemical properties of **1**, **2** and **3** at a glassy carbon electrode were investigated using cyclic voltammetry in aqueous solutions having pH values between 2 and 9. The cyclic voltammograms of **1** (figure 6(a)) at pH 2.22 exhibit a pair of waves with $E_a = 0.02$ V and $E_c = -0.10$ V *versus* SCE; $\Delta E_p = 120$ mV (where E_a and E_c are the anodic and cathodic peak potentials and ΔE_p is the potential separation between the peaks), attributed to redox processes centered on the metal (Cu^{II}/Cu^{I}). An increase in pH promotes the disappearance of this pair of waves (Cu^{II}/Cu^{I}). Analogous to the PD system, a pair of waves with $E_a = 0.28$ V and $E_c = 0.20$ V, $\Delta E_p = 80$ mV can be assigned to the two one-electron redox of coordinated PD [11]. The electrochemical response is sensitive to the pH, and the waves shift to more negative potentials as the pH is increased. When the pH is raised to 4.18, an anodic wave appears at 0.2 V, which can be assigned to the metal centered oxidation. In acidic medium, there is an overlap of anodic peaks of $Cu^{II/III}$ and PD [20].

As shown in figure 6(b), the cyclic voltammogram of **2** at pH 2.2 exhibits a reductive wave with $E_c = -0.043$ V *versus* SCE (where E_c is the cathodic peak potential), attributed to reduction centered on the metal (Cu^{II}/Cu^{I}). With increasing pH, the location of the wave is invariable. Analogous to the PD system, a pair of waves with $E_a = 0.279$ V and $E_c = 0.191$ V; $\Delta E_p = 88$ mV can be assigned to the two one-electron redox reactions of coordinated PD. The electrochemical response is sensitive to the pH, and the waves shift to more negative potentials as pH is increased. When the pH is 8.99, redox peaks move to -0.177 V and -0.258 V. In addition, an anodic wave appears at

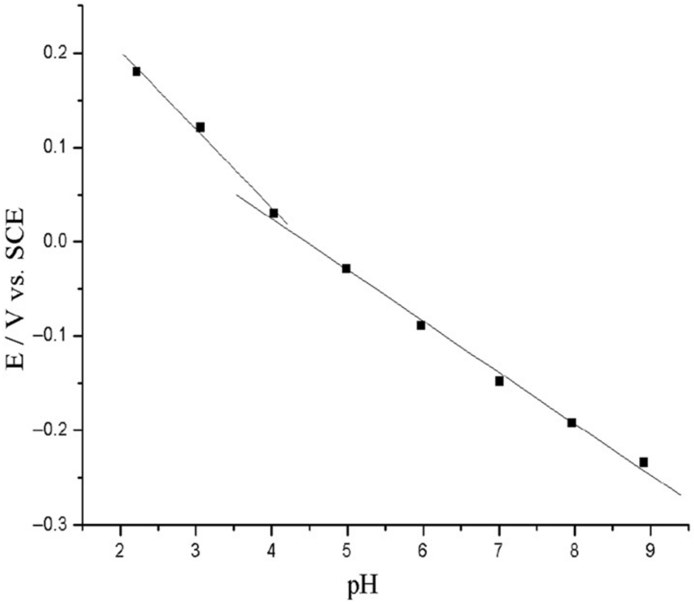

Figure 5. Plots of E_c (*vs.* SCE) *vs.* pH for the reduction of PD.

0.210 V, which can be assigned to the metal centered irreversible oxidation. In acidic medium, there is an overlap of anodic peaks of $Cu^{II/III}$ and PD.

The cyclic voltammograms of **3** [see figure 6(c)] show only one redox couple assigned to the ligand-centered reduction/oxidation processes and with the pH increasing, the redox couple becomes two redox couple waves. Figure 7(a), (b) and (c) show the plots of E_c values of **1**, **2** and **3** against pH. The slopes of the three figures are roughly −50, −66, −56 mV/pH, respectively, indicating that reduction of PD proceeded via the $2e^-/2H^+$ processes. By comparing the slope of the free ligand, the distinct behavior of the complexes is apparent [20]. The transformation is probably brought by the coordination of PD ligand.

4. Conclusion

Three complexes of 1,10-phenanthroline-5,6-dione ligand $[Cu(PD)_3]. (ClO_4)_2 \cdot 2.25CH_3CN \cdot 6H_2O$ (**1**), $[Cu(PD)(DMSO)Cl_2] \cdot DMSO \cdot H_2O$ (**2**) and $[Co(PD)_3](ClO_4)_2 \cdot CH_3CN \cdot 2H_2O$ (**3**) have been synthesized and characterized. The crystal structure of **2** shows Cu(II) in a distorted square pyramidal geometry, **1** and **3** are distorted octahedra. The electrochemical properties of these complexes are pH-dependent and the reduction of coordinated PD

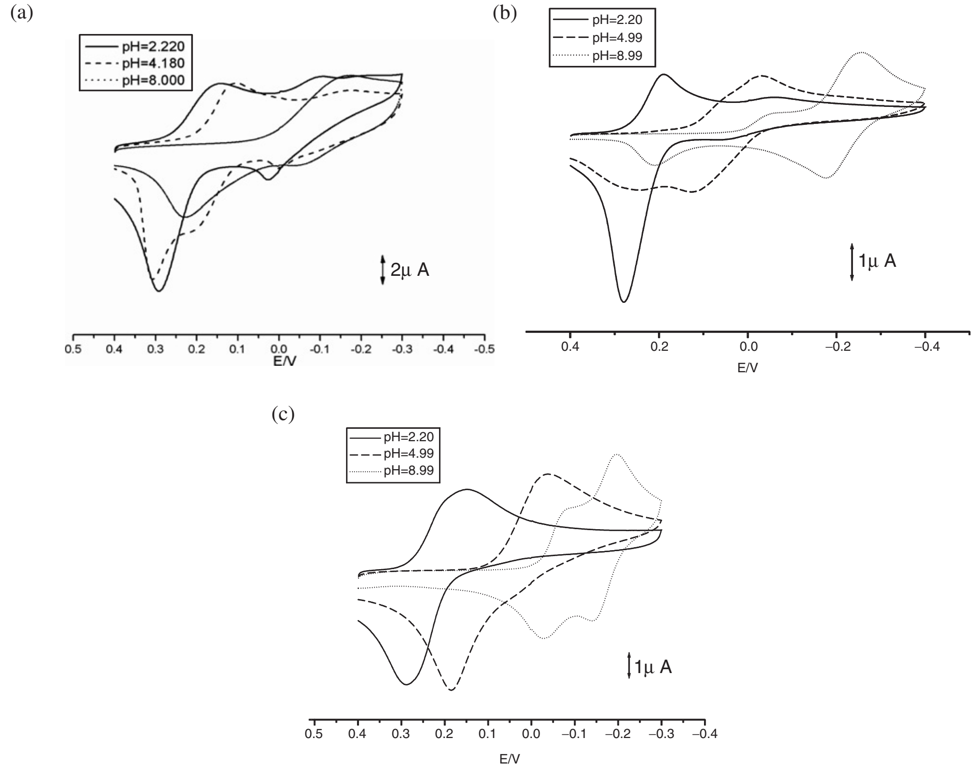

Figure 6. Cyclic voltammograms of **1**(a), **2**(b) and **3**(c) in 0.1 mol L^{-1} phosphate buffer solutions at several pH values.

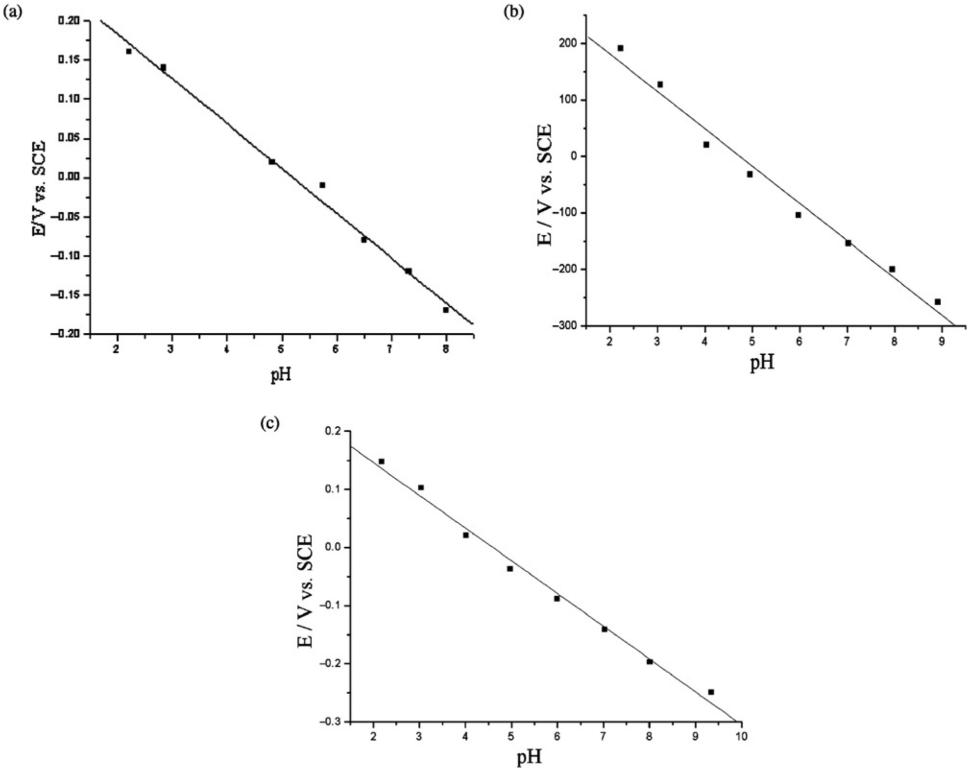

Figure 7. Plots of E_c (*vs.* SCE) *vs.* pH for the reduction of **1**(a), **2**(b) and **3**(c).

proceeded via $2e^-/2H^+$ processes. This behavior could be important for research into electrochemical properties and the influence of acidity of dioxolene ligands. This research is useful to modeling the mechanism of proton pumping in the Cytochrome *c* oxidase by model compounds.

Supplementary information

Crystallographic data for the structures reported in this article have been deposited with the Cambridge Crystallographic Data Centre, CCDC No. **1**: 607011; **2**: 645217. Copies of the data can be obtained free of charge on application to CCDC (Email: deposit@ccdc.cam.ac.uk or http://www.ccdc.cam.ac.uk).

Acknowledgement

This work was supported financially by the National Science Foundation of China (Grant No. 20331020).

References

[1] C.G. Pierpont. *Coord. Chem. Rev.*, **216–217**, 99 (2001).
[2] C.G. Pierpont, C.W. Lange. *Inorg. Chim. Acta*, **263**, 219 (1997).
[3] C.G. Pierpont, R.M. Buchanan. *Coord. Chem. Rev.*, **38**, 45 (1981).
[4] A. Dei, D. Gatteachi, L. Pardi. *Inorg. Chem.*, **29**, 1442 (1990).
[5] P.R. Auburn, A.B.P. Lever. *Inorg. Chem.*, **29**, 2551 (1990).
[6] S. Emt, P. Hanel, J. Jordanov, W. Kaim, V. Kasack, E. Roth. *J. Am. Chem. Soc.*, **111**, 1733 (1989).
[7] R.M. Buchanan, C.G. Pierpont. *J. Am. Chem. Soc.*, **102**, 4951 (1980).
[8] M.W. Lynch, D.N. Hendrickson, B.J. Fitzgerald, C.G. Pierpont. *J. Am. Chem. Soc.*, **106**, 2041 (1984).
[9] G.A. Fox, S. Bhattacharya, C.G. Pierpont. *Inorg. Chem.*, **30**, 2895 (1991).
[10] Q. Wu, M. Maskus, F. Pariente, F. Tobalina. *Anal. Chem.*, **68**, 3688 (1996).
[11] C.A. Goss, H.D. Abruna. *Inorg. Chem.*, **24**, 4263 (1985).
[12] G.M. Sheldrick. *Correction Software*, University of Göttingen, Germany (1996).
[13] G.M. Sheldrick. *SHELXS 97, Program for the Solution of Crystal Structures*, University of Göttingen, Germany (1997).
[14] G.M. Sheldrick. *SHELXL 97, Program for the Refinement of Crystal Structures*, University of Göttingen, Germany (1997).
[15] Z. Zhang, W. Yan, M. Fan. *Appl. Chem.*, **22**, 103 (2005).
[16] G. Hilt, T. Jarbawi, W.R. Haineman, E. Steckhan. *Chem. Eur. J.*, **3**, 79 (1997).
[17] P. Zanello. *Inorganic Electrochemistry, Theory, Practice and Application*, p. 104, The Royal Society of Chemistry, London (2003).
[18] P. Zanello. *Inorganic Electrochemistry: Theory, Practice and Applicationc*, p. 25, The Royal Society of Chemistry, London (2003).
[19] Y. Lei, F.C. Anson. *J. Am. Chem. Soc.*, **117**, 9849 (1995).
[20] G.J. Xu, Y.Y. Kou, L. Feng, S.P. Yan, D.Z. Liao, Z.H. Jiang, P. Cheng. *Appl. Organomet. Chem.*, **20**, 351 (2006).